

Perceptual Propagation - Episode VI: Return of the Psychoacoustic Kick-Ass

Chris Malloy and Aidos Abzhanov
University of North Carolina at Chapel Hill

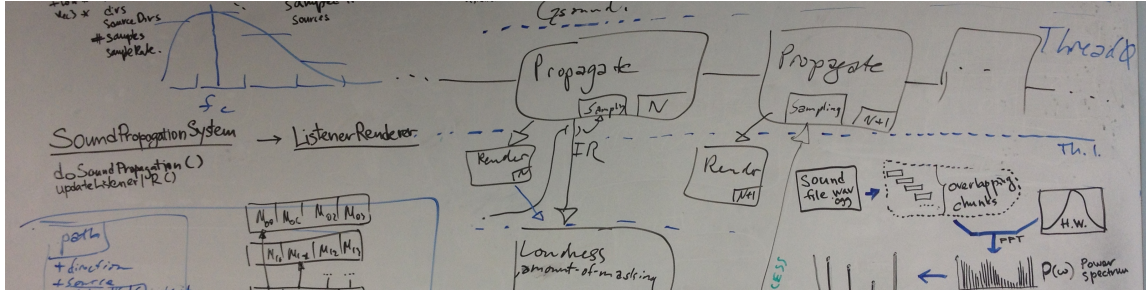


Figure 1: The System Design.

Abstract

We introduce a new method for optimizing the performance of path-based sound propagation phase of 3D audio simulation system by leveraging the perceptual feedback from the auralization (and rendering) stage. Our method combines using of psychoacoustics measures to prioritize perceptually important paths and guiding the ray tracing algorithm to better distribute rays to sources ...

CR Categories: I.3.5 [Computer Graphics]: Computational Geometry and Object Modeling—Physically based modeling I.3.5 [Computer Graphics]: Applications—Sound rendering;

Keywords: sound propagation, perceptual importance sampling

1 Introduction

This project aims to produce auditory display pipeline with perceptually optimal sound propagation component (subsystem, state). We force a simulator to focus its computational resources on the perceptually salient regions of an audio (aural/sound) scene, while maintaining the high (same) level of perceptual quality and remaining computationally efficient.

The sound simulation is important area of research and application. Interactive sound simulation is used in many field (games, VR, architectural acoustics). Computation of the sound propagation in complex scenes is either expensive or imprecise. Wave based sound propagation methods can produce accurate results [?], but take too much time to be considered for real-time applications. Geometry based methods, on the other hand, provide fast, but approximate

solution to the wave equation. The accuracy of geometric (ray-based) approaches can be improved by shooting (generating) more rays (paths), however this directly correlates with the computation time of the simulation. The core idea of our project is to exploit the perceptual limitations of the human auditory system to shoot the rays robustly.

[Small intro on perceptual part ...] It is reasonable to use this psychoacoustic principles to guide the propagation system during ray sampling phase.

We introduce a combination of techniques that improve the running time or/and perceptual quality of the sound propagation system. We first compute perceptual loudness corresponding to the sound signal and the impulse response (IR) of each path from the listener to the sound source. We next use the directional information of the paths to generate spherical distribution of a loudness around the listener, which, combined with HRTF, characterizes how an ear receives a sound from a point in space. We finally integrate the spherical loudness distribution into the next frame's sampling strategy.

Concretely, following are the contributions of our project work:

- a novel approach of using the psychoacoustic principles during the sound propagation stage;
- a new technique for constructing loudness distribution map;
- a partial preprocessing of the perceptual information for maintain real-time level of computations.
- an implementation the proposed methods and integration of them into gSound, an interactive sound propagation and rendering system.

Operating together these contributions constitute a system that can produce a Jedi from any hopeless Padawan.

2 Related Work

Our work is based on ray-tracing methods of sound propagation simulation, and psychoacoustic principles of human auditory system. In this section we give brief overview of related work in geometric sound propagation, perceptual coding, and perceptual audio rendering.

Geometric Sound Propagation [Sound Simulation pipeline overview? short: synthesis, propagation and rendering (diagram).]

There are two main approaches in solving the problem of sound propagation: wave-based [?; ?; ?] and geometric [?], with an accuracy and computational complexity being the major trade-offs between them. In wave-based approach the acoustic wave equation is solved numerically, while in geometric approach the problem is reduced to geometric computations assuming the rectilinear propagation of sound waves. Due to the high computational demands of wave-based methods, the field of interactive sound propagation algorithms is primarily dominated by geometric methods, although there are interactive wave-based methods for static scenes [?; ?].

Geometric approach includes algorithms based on image source [?], beam tracing [?], frustum tracing [?], ray tracing [?; ?]. Recent advances in ray tracing based approach together with its highly parallel nature makes it stand out among other geometric approaches for interactive sound [auralization (simulation)] applications [?; ?]. The general idea behind ray tracing based algorithms is to model sound propagation effect by considering different paths between a source and a listener. These propagation paths encode information about the delays and attenuations of sound traveling along the paths, and may consist of any number of reflections and diffractions.

See [?] for a more comprehensive survey on acoustic rendering and auditory.

Psychoacoustics When sound wave reaches human ear the mechanical energy transforms into neural signal [pulse?], which eventually travels to the brain. This [what?] suggests that taking into account the final signal transformations due to ear and brain may be advantageous for some sound processing applications.

The field of psychoacoustics has made significant progress toward characterizing the time-frequency analysis capabilities of the inner ear [?]. One of the vivid examples of applying psychoacoustic principles to digital signal processing is perceptual coding. It exploits the human auditory system's inability to hear quantization noise under condition of auditory masking [?] to perform perceptually lossless audio signal compression [?]. These were applied to different audio compression formats, including MPEG-1 Audio Layer III (MP3).

The main psychoacoustic principles consist of absolute hearing thresholds, critical band frequency analysis, simultaneous masking, the spread of masking, and temporal masking. Making use of these psychoacoustic notions in the audio simulation system allows ...

Perceptual Audio Rendering Our work is related to the work of [?], where the psychoacoustic principles are utilized to handle large number of sources and accelerate sound rendering. Similar approach was done in [?] for producing scalable or progressive rendering of complex mixtures of sounds. Our work differs from the previous two in that we intend to leverage psychoacoustic feedback throughout the entire pipeline (including propagation), not only in rendering phase or for clustering.

Spherical Projection Testing. Cite it! Right here, Right now!

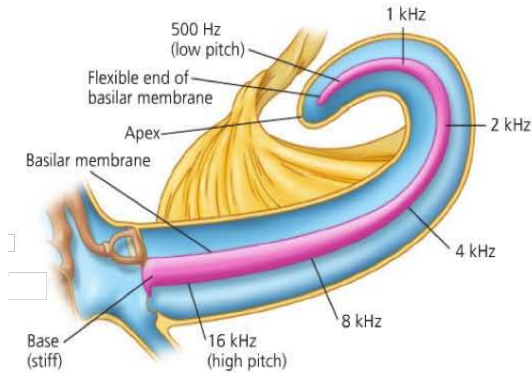


Figure 2: The basilar membrane

3 Introduction to Psychoacoustics

Psychoacoustics is the science of auditory perception and the human experience of hearing. Limitations induced by the psychological and physiological mechanisms responsible for hearing are of particular interest and have been successfully applied to musical composition, architecture, digital audio coding, and mixing/rendering sound. Individual psychoacoustic effects and illusions are referred to as *psychoacoustic principles* and include:

- The Absolute Threshold of Hearing
- Critical Band Frequency Analysis
- Simultaneous Masking
- Non-Simultaneous Masking
- The Spread of Masking

In this method we seek to demonstrate how these basic psychoacoustic principles can be leveraged in a geometric sound propagation pipeline, with our most novel contribution being the use of masking in the propagation phase of sound simulation.

Auditory Filters and the Bark Scale of Critical Bandwidths The perception of sound frequency is mediated by the **basilar membrane**, a coiled structure of the inner ear that vibrates in response to sound energy. Regions of the basilar membrane have a characteristic frequency they are most sensitive to. This characteristic frequency is highest at the base of the basilar membrane and continuously decreases along its length.

Pure tones result in patterns of excitation on the basilar membrane that may overlap for sounds that are nearby in frequency, and for this reason the basilar membrane is abstracted in literature as a bank of overlapping **auditory filters**. The **Bark frequency scale** is measured in units of the frequency-dependent bandwidths of the auditory filters of the basilar membrane, referred to as the **critical bandwidths**, and is a commonly used frequency scale in psychoacoustics because it is directly proportional to the frequency resolution of human hearing.

Spectral Masking Because of the observed overlap of auditory filters, a loud tone will also excite regions of the basilar membrane that should correspond to neighboring frequencies. This interference of excitation is the phenomenon of **spectral masking**, where

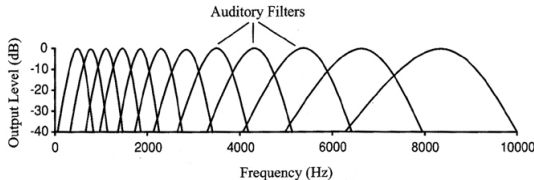


Figure 3: Curves representing the response of auditory filters as a function of center frequency

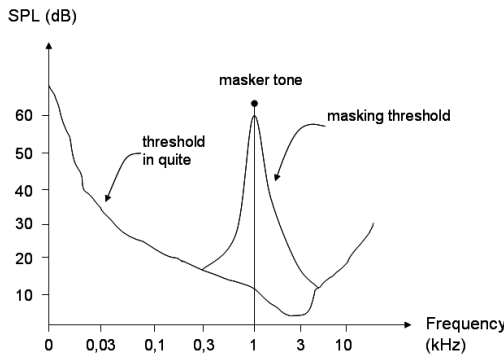


Figure 4: Absolute threshold of hearing and masked threshold

a tone played at a given frequency will perceptually occlude relatively softer tones that are nearby in frequency. The intensity of masking is asymmetric in frequency with lower tones masking higher tones with a higher intensity than the reverse. This psychoacoustic principle has been referred to as **the upward spread of masking** (the axis of ‘upward’ being frequency).

The **absolute threshold of hearing** is a curve of minimum pressure level necessary to perceive a sound at a given frequency and in the presence of relative quiet. Similarly, a **masking threshold** characterizes the threshold below which a sound is made imperceptible in the presence of a masker. The net result of spectral masking in the presence of multiple tones is approximately additive, and the net amount of masking continues to effect later tones after the masking tone has ended because of a phenomenon referred to as **non-simultaneous or temporal masking**.

4 MPEG Psychoacoustic Models

The MPEG-1 audio standard specifies an algorithm for compressing digital audio signals by removing the perceptually inaudible components. The standard defines two psychoacoustic models that model the human sound perception system and inform the quantization of individual audio blocks during compression. The models differ in computational complexity, but share the main idea of splitting sound into tone-masking-noise and noise-masking-tone, and calculating a global masking threshold curve by combining the two individual models based on how tonal or noise-like the signal is. This global masking threshold represents the minimal sound power perceptible by the average human listener. The global threshold guides the encoders allocation of bits to better represent an error-free signal. In the psychoacoustic model 1 the tonality of a component is determined from peaks in the critical bands, while in the model 2, it is determined using a predictability measure.

The psychoacoustic models involve following main steps of the

global masking threshold computation:

- Spectral Analysis: calculation of the *power spectral density* (PSD) which describes the distribution of the power of a signal over the different frequencies.
- Critical Band Analysis: the power spectrum of the signal is partitioned into critical bands by integrating over the corresponding bandwidths.
- Tonality Analysis: the *spectral flatness measure* (SFM) is used to characterize the spectrum of the signal. The SFM is defined as the ratio of the geometric to arithmetic mean values of power spectral density. The *tonality index* (TI) is calculated by comparing estimated SFM with the SFM of a sinusoidal signal. Values of the tonality index that are closer to zero indicate that the spectrum of the signal look similar to a spectrum of white noise. Values of TI that are closer to one indicate that the spectral power is concentrated in a relatively small number of bands and the signal sounds like a mixture of sine waves.
- Masking Analysis: The masking threshold is determined by calculating an offset to the excitation pattern. Due to asymmetry of tone and noise maskings the value of offset depends on the value of the tonality index. The final values for the offset are interpolated from the offsets for tone-like and noise-like signals.
- Spread of Masking: Inter-band masking is taken into account by convolving each of the maskers with the *spreading function*.

5 Overview

The general (high-level) description of the algorithm here.

Spectral Masking Masking thresholds are obtained by performing critical band analysis (with spreading), making a determination of the noise-like or tone-like nature of the signal, applying thresholding rules for the signal quality, then accounting for the absolute hearing threshold [?]. We assume that the input sound samples are given in advance, and can be pre-processed to extract spectral information about the signal. N samples long Hann window with 50 percent overlap is used to produce the parts of the input sound signal that are processed by psychoacoustic module.

The short time spectrum $X(\omega)$ is computed from the windowed signal chunk $x(i)$ $i \in [0, N - 1]$ using discrete Fourier transform. From this we generate the *power density spectrum* by

$$P(\omega) = Re(X(\omega))^2 + Im(X(\omega))^2, \quad \omega \in [0, N - 1].$$

Signal power for each critical band i is calculated by summing corresponding power density spectra within that frequency band

$$B_i = \sum_{\omega=\omega_{i,low}}^{\omega_{i,high}} P(\omega).$$

To account for spreading of masking the critical band signal power is convolved

$$C_i = B_i * SF_i$$

with the *spreading function* SF_i , representing masking across critical bands and given by analytical expression:

$$SF_i = 15.81 + 7.5(\delta i + 0.474) - 17.5\sqrt{1 + (\delta i + 0.474)^2}.$$

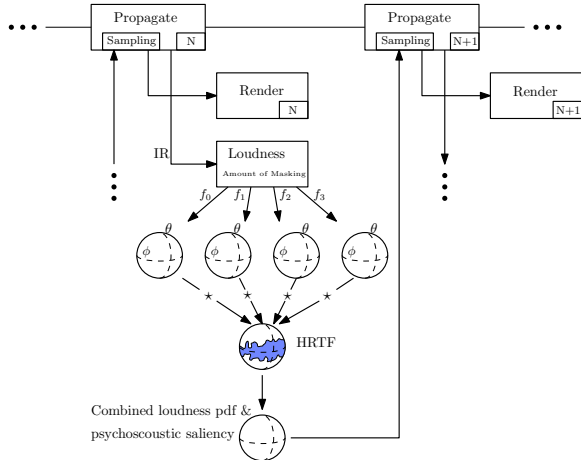


Figure 5: This is a tiger.

Due to the asymmetry of masking there are two masking thresholds: for tone masking noise the threshold is estimated as $14.5 + i$ dB below C_i , while for noise masking tone it is estimated as 5.5 dB below C_i , for each band i .

In order to recognize a tonal or noise-like signal within a certain number of samples, the *spectral flatness measure* (SFM) is estimated

$$SFM_{dB} = 10 \log_{10} \frac{\mu_g}{\mu_a},$$

where μ_g and μ_a are geometric and arithmetic means of the C_i .

The SFM is compared with the SFM of a sinusoidal signal (entirely tonelike signal with SFM = -60 dB) and the *tonality index* is calculated [?] by

$$\alpha = \min\left(\frac{SFM_{dB}}{-60}, 1\right).$$

SFM = 0 dB corresponds to a noise-like signal and leads to $\alpha = 0$, whereas an SFM = 75 dB gives a tone-like signal ($\alpha = 1$).

The tonality index is then used to weight the thresholding rules for each band to form an *offset* between signal level and the masking threshold in critical band i

$$O_i = \alpha(14.5 + i) + (1 - \alpha)5.5 \quad (\text{in dB}).$$

Finally, a set of *just noticeable difference* JND estimates in the frequency power domain are then formed by subtracting the offsets from the Bark spectral components

$$T_i = 10^{\log_{10}(C_i) - (O_i/10)}.$$

Coupling with gSound We used gSound, interactive ray-tracing based sound propagation system, to perform the testing of our algorithm, and quickly realized that it is an exceptionally good example of a tool for human torture. Especially, when combined with the MS Visual Studio IDE.

gSound [?] contain the following features: backward ray tracing, multi-source clustering, HRTF rendering capabilities.

Here we discuss the design (see Figure 5) for coupling our methodology with gSound.

Results

6 Implementation

The general pipeline of our system consists of a preprocessing step that is performed on source audio as well as a runtime component that enables feedback from the auralization of IRs computed in one step of propagation to accelerate the next step of propagation.

Preprocessing Much of the sound processing performed as part of the MPEG Psychoacoustic Model II can be precomputed given a clip of audio that will become a source of sound. We perform a short-time fourier transform of the audio using 512 sample-wide Hanning windows with a 50% overlap between neighboring windows. We store this in an augmented representation of the source's sound buffer that can interpolate between windowed spectrograms to arrive at the frequency representation of the audio corresponding to a specific path's delay and start time. Likewise, we also store and interpolate the power spectral density, tonality, and Bark critical bands precomputed from this frequency representation. When the frequency bands that will be used to discretize sound in the impulse response are known, the spreading function used in excitation and masking computations as well as the offsets corresponding to noise-masking-tone and tone-masking-noise can also be precomputed. As is also done in the Psychoacoustic Model II and the work of Nikolas et al, we assume a negligible effect due to noise-masking-noise and that the global masking threshold is adequately characterized by only the former two.

Perceptual Salience Given an impulse response corresponding to propagation step n of the simulation, we compute a measure of perceptual salience based on the directionality of loudness and the amount of masking between sampled paths that are nearby in time and frequency. We assume temporal locality of the IR and use this measure of salience as prior knowledge to accelerate step $n + 1$ of the propagation system.

For each path of an IR from propagation step n , we use its associated delay to retrieve the precomputed tonality and power spectral density of the source's sound at that time. We then compute its excitation pattern by convolving the precomputed spreading function with the path's power spectral density and frequency-binned response. We also compute for each path its contribution to the masking threshold of hearing by combining the tone-masking-noise and noise-masking-tone models based on tonality of the signal and store this as an array of frequency binned thresholds sampled in time.

We assume the perceptual salience of a direction from the listener is proportional to the excitation from that direction above the masking threshold. We therefore compute our measure of salience as the amount of excitation from that direction above the corresponding threshold associated with the path's delay. The salience of each path is then rasterized onto a spherical mapping of a grid representing directions about the listener. Because we are sampling discrete, possibly sparse, paths onto a spherical function that will ultimately be used as a probability density function, we rasterize the path's salience onto the sphere using a gaussian kernel instead of the nearest cell (as is done in kernel density estimation).

Path Sampling Paths at propagation step $n + 1$ are sampled around the listener by Monte-Carlo sampling of the spherical salience function generated from the IR of propagation step n . The probability of sampling a path from a given direction becomes proportional to the normalized salience in that direction and the path's sound power is then inversely scaled by the normalized salience as

a bias correction. As a result, paths that are perceptually negligible in their contribution to the final rendered audio will be sampled less often and fewer paths will be needed to converge to an accurate IR of the scene.

gSound In our gSound implementation, we perform the per-sound precomputation as the scene is loaded and combine our representation with that of the sound buffers and sources. This accounts for the bulk of processing, the remainder of which is handled per-IR. For the runtime component we have inserted our system as a separate IR update job running in the same threadpool as the main system that is executed for each freshly computed IR. The current salience measure is used in propagation as the next is computed from the most recent IR and is accessible for visualization through the main propagation system.

Both the sampled and discrete path IR are used to compute salience, and so potentially numerous samples might be rasterized to the sphere as a result. We therefore perform the kernel density estimation of spherical functions by rasterizing each discrete sample to its nearest cell and performing several box filters to approximate a gaussian kernel as a post-processing step. This approach is much more efficient than rasterizing individual gaussian functions and produces similar results. In order to avoid distortion from box filtering the 2d grid directly, our spherical mapping is a per-hemisphere Lambert cylindrical projection.

7 Conclusion and Outlook

Evaluate the existing efficiency of the pipeline based on the distribution of paths in the existing renderer. Conduct user study.

Decouple the propagation to include both backward and forward paths (carrying importance and source information respectively)

Try strategies to connect the paths and guide sampling on both ends to converge more efficiently

Improve sampling schemes based on the state-of-the-art algorithms from graphics field.

Binaural masking.

Incorporate the support of temporal masking (forward, backward)

Go deeper into Rendering part of the system (how can we use psychoacoustic principles there)

Acknowledgements

To Celeste, for the pizza and coffee, and Hasan, for all the bagels.

References

- AMBIKAIRAJAH, E., DAVIS, A., AND WONG, W. 1997. Auditory masking and mpeg-1 audio compression. *Electronics & communication engineering journal* 9, 4, 165–175.
- BORISH, J. 1984. Extension of the image model to arbitrary polyhedra. *The Journal of the Acoustical Society of America* 75, 6, 1827–1836.
- CHANDAK, A., ANTANI, L., TAYLOR, M., AND MANOCHA, D. 2009. Fastv: From-point visibility culling on complex models. In *Computer Graphics Forum*, vol. 28, Wiley Online Library, 1237–1246.

FUNKHOUSER, T., CARLBOM, I., ELKO, G., PINGALI, G., SONDHI, M., AND WEST, J. 1998. A beam tracing approach to acoustic modeling for interactive virtual environments. In *Proceedings of the 25th annual conference on Computer graphics and interactive techniques*, ACM, 21–32.

FUNKHOUSER, T., TSINGOS, N., AND JOT, J.-M. 2003. Survey of methods for modeling sound propagation in interactive virtual environment systems.

GUMEROV, N. A., AND DURAISWAMI, R. 2009. Wideband fast multipole accelerated boundary element methods for the three-dimensional helmholtz equation. *The Journal of the Acoustical Society of America* 125, 4, 2566–2566.

HULUSIC, V., HARVEY, C., DEBATTISTA, K., TSINGOS, N., WALKER, S., HOWARD, D., AND CHALMERS, A. 2012. Acoustic rendering and auditory–visual cross-modal perception and interaction. In *Computer Graphics Forum*, vol. 31, Wiley Online Library, 102–131.

JOHNSTON, J. D. 1988. Estimation of perceptual entropy using noise masking criteria. In *Acoustics, Speech, and Signal Processing, 1988. ICASSP-88., 1988 International Conference on*, IEEE, 2524–2527.

KIRK, A. G., AND O'BRIEN, J. F. 2011. Perceptually based tone mapping for low-light conditions. *ACM Trans. Graph.* 30, 4, 42.

MANOCHA, D., AND LIN, M. C. 2009. Interactive sound rendering. In *Computer-Aided Design and Computer Graphics, 2009. CAD/Graphics' 09. 11th IEEE International Conference on*, IEEE, 19–26.

MEHRA, R., RAGHUVANSHI, N., ANTANI, L., CHANDAK, A., CURTIS, S., AND MANOCHA, D. 2013. Wave-based sound propagation in large open scenes using an equivalent source formulation. *ACM Transactions on Graphics (TOG)* 32, 2, 19.

MOECK, T., BONNEEL, N., TSINGOS, N., DRETTAKIS, G., VIAUD-DELMON, I., AND ALLOZA, D. 2007. Progressive perceptual audio rendering of complex scenes. In *Proceedings of the 2007 symposium on Interactive 3D graphics and games*, ACM, 189–196.

PAINTER, T., AND SPANIAS, A. 2000. Perceptual coding of digital audio. *Proceedings of the IEEE* 88, 4, 451–515.

PAN, D. 1995. A tutorial on mpeg/audio compression. *IEEE multimedia* 2, 2, 60–74.

RAGHUVANSHI, N., SNYDER, J., MEHRA, R., LIN, M., AND GOVINDARAJU, N. 2010. Precomputed wave simulation for real-time sound propagation of dynamic sources in complex scenes. In *ACM Transactions on Graphics (TOG)*, vol. 29, ACM, 68.

SAVIOJA, L. 2010. Real-time 3d finite-difference time-domain simulation of low-and mid-frequency room acoustics. In *13th Int. Conf on Digital Audio Effects*, vol. 1, 75.

SCHISSLER, C., AND MANOCHA, D. 2011. Gsound: Interactive sound propagation for games. In *Audio Engineering Society Conference: 41st International Conference: Audio for Games*, Audio Engineering Society.

SCHISSLER, C., AND MANOCHA, D. 2015. Interactive sound propagation and rendering for large multi-source scenes.

SCHISSLER, C., MEHRA, R., AND MANOCHA, D. 2014. High-order diffraction and diffuse reflections for interactive sound

propagation in large environments. *ACM Transactions on Graphics (SIGGRAPH 2014)* 33, 4, 39.

STUART, J. R. 1996. The psychoacoustics of multichannel audio. In *Audio Engineering Society Conference: UK 11th Conference: Audio for New Media (ANM)*, Audio Engineering Society.

TAYLOR, M., CHANDAK, A., MO, Q., LAUTERBACH, C., SCHISSLER, C., AND MANOCHA, D. 2010. i-sound: Interactive gpu-based sound auralization in dynamic scenes. Tech. rep., Tech. Rep. TR10-006.

TAYLOR, M., CHANDAK, A., MO, Q., LAUTERBACH, C., SCHISSLER, C., AND MANOCHA, D. 2012. Guided multi-view ray tracing for fast auralization. *Visualization and Computer Graphics, IEEE Transactions on* 18, 11, 1797–1810.

THOMPSON, L. L. 2006. A review of finite-element methods for time-harmonic acoustics. *J. Acoust. Soc. Am* 119, 3, 1315–1330.

TSINGOS, N., FUNKHOUSER, T., NGAN, A., AND CARLBOM, I. 2001. Modeling acoustics in virtual environments using the uniform theory of diffraction. In *Proceedings of the 28th annual conference on Computer graphics and interactive techniques*, ACM, 545–552.

TSINGOS, N., GALLO, E., AND DRETTAKIS, G. 2004. Perceptual audio rendering of complex virtual environments. In *ACM Transactions on Graphics (TOG)*, vol. 23, ACM, 249–258.

TSINGOS, N. 2005. Scalable perceptual mixing and filtering of audio signals using an augmented spectral representation. In *8th International Conference on Digital Audio Effects (DAFx 2005)*, 6.